

Dynamical Coupled-Channel Analysis at EBAC

T. -S. H. Lee^{1,2}

¹ Physics Division, Argonne National Laboratory, Argonne, IL 60439

² Excited Baryon Analysis Center (EBAC), Thomas Jefferson National Accelerator Facility, Newport News, Va. 22901

Received: date / Revised version: date

Abstract. The status of the dynamical coupled-channel analysis at EBAC is reported.

PACS. 1 3.75.Gx, 13.60.Le, 14.20.Gk

1 Introduction

In this contribution, we report on the dynamical coupled-channel analysis being pursued at the Excited Baryon Analysis Center (EBAC) of Jefferson Laboratory. EBAC was established in January, 2006. Its objective is to extract the parameters associated with the excited states (N^*) of the nucleon from the world data of meson production reactions, and to also develop theoretical interpretations of the extracted N^* parameters.

Since N^* states are unstable, their structure must couple with the reaction channels in the meson production reactions. To determine correctly the spectrum of N^* states, an analysis of the meson production data must account for the coupled-channel unitary condition. The extracted N^* parameters can be interpreted correctly only when the reaction mechanisms in the short-range region where we want to map out the N^* structure have been accounted for. To meet these two crucial requirements, the dynamical coupled-channel model developed in Ref.[1] is being applied at EBAC to analyze the data of π , $\pi\pi$, η , K , and ω production. It involves solving the following coupled integral equations

$$T_{\alpha,\beta}(p_\alpha, p_\beta; E) = V_{\alpha,\beta}(p_\alpha, p_\beta) + \sum_\gamma \int_0^\infty dp' V_{\alpha,\gamma}(p_\alpha, p') G_\gamma(p', E) T_{\gamma,\beta}(p', p_\beta, E), \quad (1)$$

$$V_{\alpha,\beta} = v_{\alpha,\beta} + \sum_{N^*} \frac{\Gamma_{N^*,\alpha}^\dagger \Gamma_{N^*,\beta}}{E - M^*}, \quad (2)$$

where $\alpha, \beta, \gamma = \gamma N, \pi N, \eta N, \text{ and } \pi\pi N$ which has $\pi\Delta, \rho N, \sigma N$ resonant components, $G_\gamma(p, E)$ is the propagator of channel γ , $v_{\alpha,\beta}$ is defined by meson-exchange mechanisms, and $\Gamma_{N^*,\beta}$ is related to the quark-gluon sub-structure of N^* . At the present time, it is reasonable to interpret $\Gamma_{N^*,\beta}$ in terms of hadron structure calculations with effective degrees of freedom, such as the constituent quark model[2] and the model[3] based on Dyson-Schwinger Equations. In

the near future, one hopes to relate $\Gamma_{N^*,\beta}$ to Lattice QCD (LQCD) calculations.

If we take the on-shell approximation, Eq.(1) is reduced into an algebraic form of K-matrix models[4,5,6,7]

$$T_{\alpha,\beta}^k(p_\alpha, p_\beta, E) = \sum_\gamma V_{\alpha,\gamma}(p_\alpha, p_\gamma) \times [\delta_{\alpha,\gamma} + i\rho(p_\gamma) T_{\gamma,\beta}^k(p_\gamma, p_\beta, E)], \quad (3)$$

where $\rho(p_\gamma)$ is an appropriate phase space factor. Qualitatively speaking, the use of the on-shell model based on $T_{\alpha,\beta}^k(p_\alpha, p_\beta, E)$ of Eq.(3) is to avoid an explicit treatment of the reaction mechanisms in short range region where we want to map out the quark-gluon sub-structure of N^* states. Thus the N^* parameters extracted by using Eq.(1) can be more directly interpreted in terms of the quark-gluon sub-structure of N^* .

In section 2, we briefly review the dynamical coupled-channel model of Ref.[1]. The recent results from EBAC are reported in section 3. Section 4 gives an outlook of EBAC.

2 Dynamical Coupled-Channel Model

Within the formulation of Ref.[1], Eqs.(1)-(2) are derived from the following Hamiltonian

$$H = H_0 + H_I \quad (4)$$

$$H_0 = \sum_{MB} [\sqrt{m_B^2 + k^2} + \sqrt{m_M^2 + p^2}] \quad (5)$$

$$H_I = \Gamma_V + v_{22} + v_{23} + v_{33} \quad (6)$$

The non-resonant interactions v_{22}, v_{23}, v_{33} are derived from phenomenological Lagrangians by using an unitary

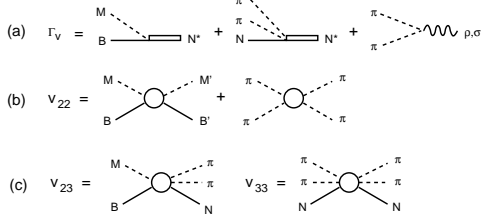


Fig. 1. Basic mechanisms of the Model Hamiltonian defined in Eqs.(4)-(6).

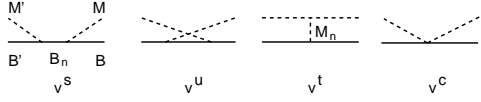


Fig. 2. Meson-baryon (MB) interaction mechanisms of $v_{2,2}$ of Eq.(6).

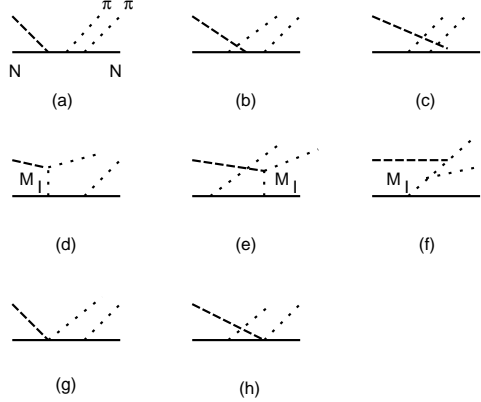


Fig. 3. Examples of non-resonant mechanisms of $v_{MN, \pi\pi N}$ with $M = \pi$ or γ (denoted by long-dashed lines). M_I denotes the intermediate mesons (π, ρ, ω).

transformation method[9,10]. The interaction v_{22} is defined by the tree diagrams, as illustrated in Fig.2. Examples of non-resonant mechanisms of v_{23} are illustrated in Fig.3. The more complex v_{33} is not included in the current analysis at EBAC.

By using the projection operator techniques, one can cast Eqs.(1)-(2) for $2 \rightarrow 2$ meson-baryon (MB) transition amplitudes into the following form

$$T_{a,b}(E) = t_{a,b}(E) + t_{a,b}^R(E), \quad (7)$$

where $a, b, c = \gamma N, \pi N, \eta N, \pi \Delta, \rho N, \sigma N$. The non-resonant amplitude in Eq.(7) is defined by

$$t_{a,b}(E) = V_{a,b} + \sum_c V_{a,c} G_c(E) t_{c,b}(E), \quad (8)$$

where the driving term is

$$V_{a,b}(E) = v_{a,b} + Z_{a,b}^{(E)}(E) + Z_{a,b}^{(I)}(E). \quad (9)$$

The effects due to the three-body unitarity cuts are included in $Z_{a,b}^{(E)}(E)$ and $Z_{a,b}^{(I)}(E)$, as illustrated in Figs.4-5.

$$Z_{MB, M'B'}^{(E)} = \frac{\Delta}{\pi} + \frac{\rho, \sigma}{N} \frac{\pi}{\Delta}$$

Fig. 4. One-particle-exchange interactions $Z_{\pi\Delta, \pi\Delta}^{(E)}$, $Z_{\rho N, \pi\Delta}^{(E)}$ and $Z_{\sigma N, \pi\Delta}^{(E)}$ of Eq.(9).

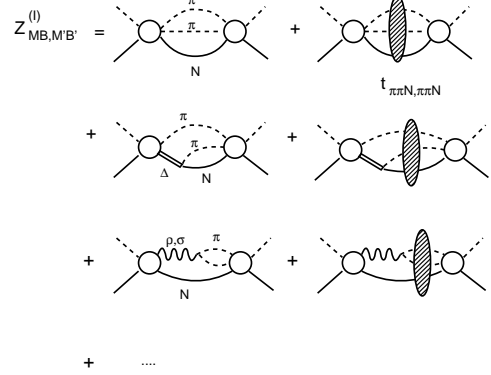


Fig. 5. Examples of mechanisms included in $Z_{MB, M'B'}^{(I)}$ of Eq.(9)

The resonant amplitude in Eq.(7) is defined by

$$t_{a,b}^R(E) = \sum_{N_i^*, N_j^*} \bar{\Gamma}_{N_i^*, a}^\dagger(E) [g(E)]_{i,j} \bar{\Gamma}_{N_j^*, b}(E), \quad (10)$$

where the dressed vertex is

$$\bar{\Gamma}_{N^*, a}(E) = \Gamma_{N^*, a} + \sum_b \Gamma_{N^*, b} G_b(E) t_{b,a}(E), \quad (11)$$

and the N^* propagator is defined by

$$g_{i,j}^{-1}(E) = E - M_i^0 \delta_{i,j} - \sum_a \bar{\Gamma}_{N_i^*, a}^\dagger G_a(E) \Gamma_{N_j^*, a}^\dagger. \quad (12)$$

Here we emphasize that the second term of the dressed vertex Eq.(11) is an necessary consequence of the unitarity condition. This term describes the meson cloud effects on the N^* excitations. See Ref.[8] for a more detailed discussion on this point.

To solve Eq.(8), we need to handle the singular structure of $Z_{a,b}^{(E)}$ and $Z_{a,b}^{(I)}$. Their matrix elements diverge within the moon-shapes region in Fig.6 and thus have singular structure illustrated in Fig.7. We overcome this difficulty by using the Spline-function method developed in Refs.[11, 12].

3 recent Results

The computer code for solving the dynamical coupled-channel equations given in section 2 has been developed. The numerical details, in particular on the use of Spline-function methods, are explained in Ref.[1].

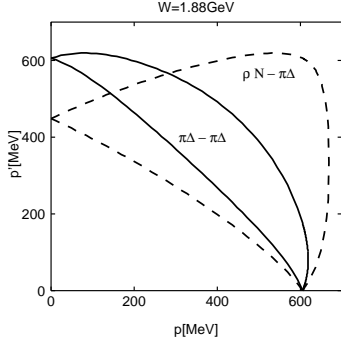


Fig. 6. Logarithmically divergent moon-shape regions of the matrix elements of $Z_{\pi\Delta, \pi\Delta}^{(E)}(p', p, E)$ (solid curves) and $Z_{\rho N, \pi\Delta}^{(E)}(p', p, E)$ (dashed curves).

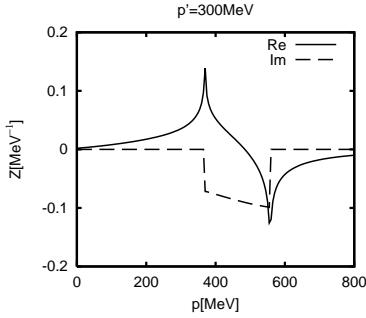


Fig. 7. Matrix elements of the one-particle-exchange term $Z_{\pi\Delta, \pi\Delta}^{(E)}(k, k', E)$ for $L = L' = 1, J = 5/2, T = 1/2$ at $k' = 300$ MeV/ c and $E = 1.88$ GeV.

Our first task is to determine the parameters of the hadronic interactions of Hamiltonian defined by Eq.(6). This has been done[13] by fitting the πN scattering data. One or two bare N^* states in each of $S, P, D,$ and F partial waves are included to generate the resonant amplitudes, defined by Eq.(10), in the fits. The parameters of the model are first determined by fitting as much as possible the empirical πN elastic scattering amplitudes of SAID[4] up to 2 GeV. Some of our fits are shown in Figs.8-9.

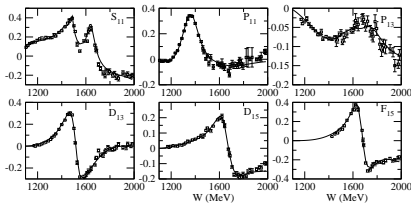


Fig. 8. Fit to the $I = \frac{1}{2} \text{Re}(T_{\pi N, \pi N})$ of SAID[4].

We then refine and confirm the resulting parameters by directly comparing the predicted differential cross section and target polarization asymmetry with the origi-

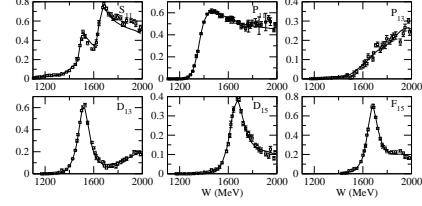


Fig. 9. Fit to the $I = \frac{1}{2} \text{Im}(T_{\pi N, \pi N})$ of SAID[4],

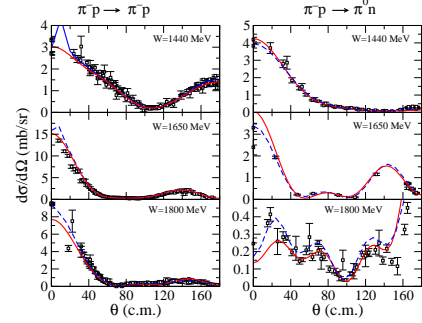


Fig. 10. Differential cross section for several different center of mass energies. Solid curves correspond to our model while blue dashed lines correspond to the SP06 solution of SAID [4]. All data have been obtained through the SAID online applications. Ref. [4].

nal data of the elastic $\pi^\pm p \rightarrow \pi^\pm p$ and charge-exchange $\pi^- p \rightarrow \pi^0 n$ processes. Typical results are shown in Fig.10. The predicted total cross sections of πN reactions are also in good agreement with the data, as shown in the left hand side of Fig.11. Our predictions of the partial total cross sections to each channel, as given in the right hand side of Fig.11, need to be refined by also fitting the $\pi N \rightarrow \pi\pi N$ data. A combined fit to both the data of πN elastic scattering and $\pi N \rightarrow \pi\pi N$ is now being pursued at EBAC. Fig.12 is a result from this very challenging task, showing the importance of the $\pi\pi N$ cut in determining the predicted invariant mass distribution of $\pi N \rightarrow \pi\pi N$ reaction. Similar pronounced effects on $\gamma N \rightarrow \pi\pi N$ reactions have been presented in Ref.[1].

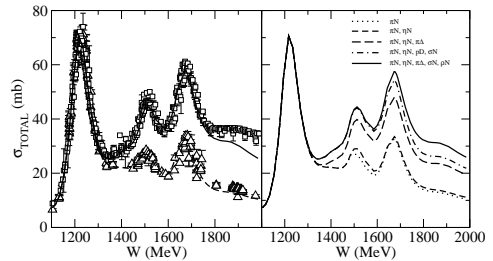


Fig. 11. Predicted $\pi^- p$ total cross sections

With the hadronic parameters determined, we are now moving to analyzing the data of electromagnetic production of π and $\pi\pi$. Here the only parameters to be de-

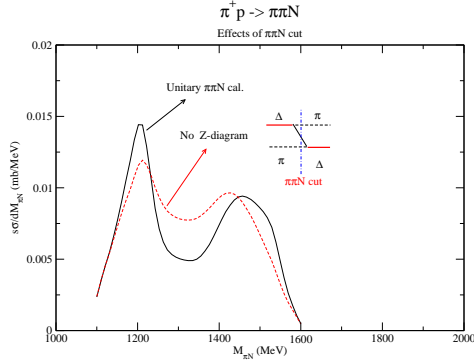


Fig. 12. The πN invariant mass distribution of $\pi N \rightarrow \pi\pi N$ reaction at $W = 1880$ MeV.

terminated are the bare $\gamma N \rightarrow N^*$ vertex interactions. In Fig.13, we show the preliminary results for $\gamma p \rightarrow \pi^+ n$. In Fig.14 we show the coupled-channel effects on the $\gamma N \rightarrow \pi N$ reactions in the Δ excitation region. More detailed results will be presented in Ref.[14].

4 Outlook

The dynamical coupled-channel model developed in Ref.[1] is being applied at EBAC to analyze the world data of meson production reactions. The analysis of π and $\pi\pi$ production data is proceeding well with some encouraging preliminary results. We have also started to analyze the data of η , K , and ω production. Here the main task is to extend the model to include the interactions associated with the $K\Lambda$, $K\Sigma$, and ωN channels.

In parallel, we are also developing an analytical continuation method to extract the resonance poles and residues from the partial wave amplitudes predicted by the constructed dynamical coupled-channel model. Furthermore, we are investigating the extent to which the resonance poles and bare N^* parameters extracted from our analysis can be related to the current hadron structure calculations; in particular the Lattice QCD calculations.

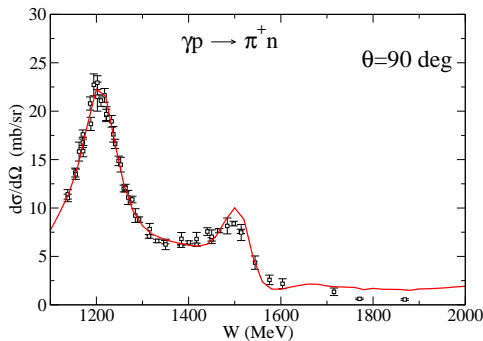


Fig. 13. Fit to the $\gamma p \rightarrow \pi^+ n$ up to $W = 2$ GeV

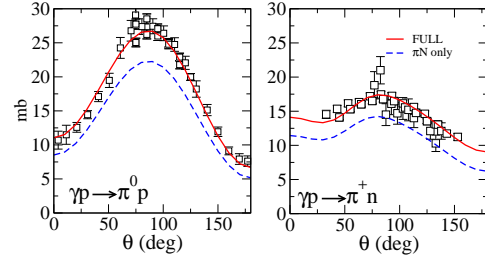


Fig. 14. Coupled-channel effects on the $\gamma N \rightarrow \pi N$ in the Δ region

This work is supported by the U.S. Department of Energy, Office of Nuclear Physics Division, under contract No. DE-AC02-06CH11357, and Contract No. DE-AC05-06OR23177 under which Jefferson Science Associates operates Jefferson Lab.

References

1. A. Matsuyama, T. Sato, T.-S. H. Lee, Phys. Rept. **439**, 193 (2007).
2. See the review by S. Capstick S and W. Roberts, *Prog. Part. Nucl. Phys.* **45** S241 (2000)
3. See the review by P. Maris and C.D. Roberts, *Int.J.Mod.Phys.* **E12** 297(2003).
4. Arndt R, Strakovsky I, Workman R, *Int. J. Mod. Phys.*, **A18** 449 (2003)
5. D. Drechsel, O. Hanstein, S. Kamalov and L. Tiator *Nucl. Phys.* **A645**, 145 (1999)
6. I. Aznauryan, *Phys. Rec.* **C71**, 01520 (2005)
7. V. Shklyar, H. Lenske, U. Mosel and G. Penner, *Phys. Rev.* **C71**, 055206 (2005)
8. B. Julia-Diaz, T.-S. H. Lee, T. Sato and L. C. Smith, *Phys. Rev. C* **75**, 015205 (2007).
9. T. Sato and T.-S. H. Lee, *Phys. Rev. C* **54**, 2660 (1996).
10. M. Kobayashi, T. Sato, and H. Ohtsubo, *Prog. Theor. Phys.* **98**, 927 (1997).
11. A. Matsuyama, *Phys. Lett.* **B152**, 42 (1984).
12. A. Matsuyama and T.-S. H. Lee, *Phys. Rev. C* **34**, 1900 (1986).
13. B. Julia-Diaz, T.-S. H. Lee, A. Matsuyama, T. Sato, to appear in *Phys. Rev. C* (2007).
14. B. Julia-Diaz, T.-S. H. Lee, A. Matsuyama, T. Sato, L.C. Smith, in preparation



(a)



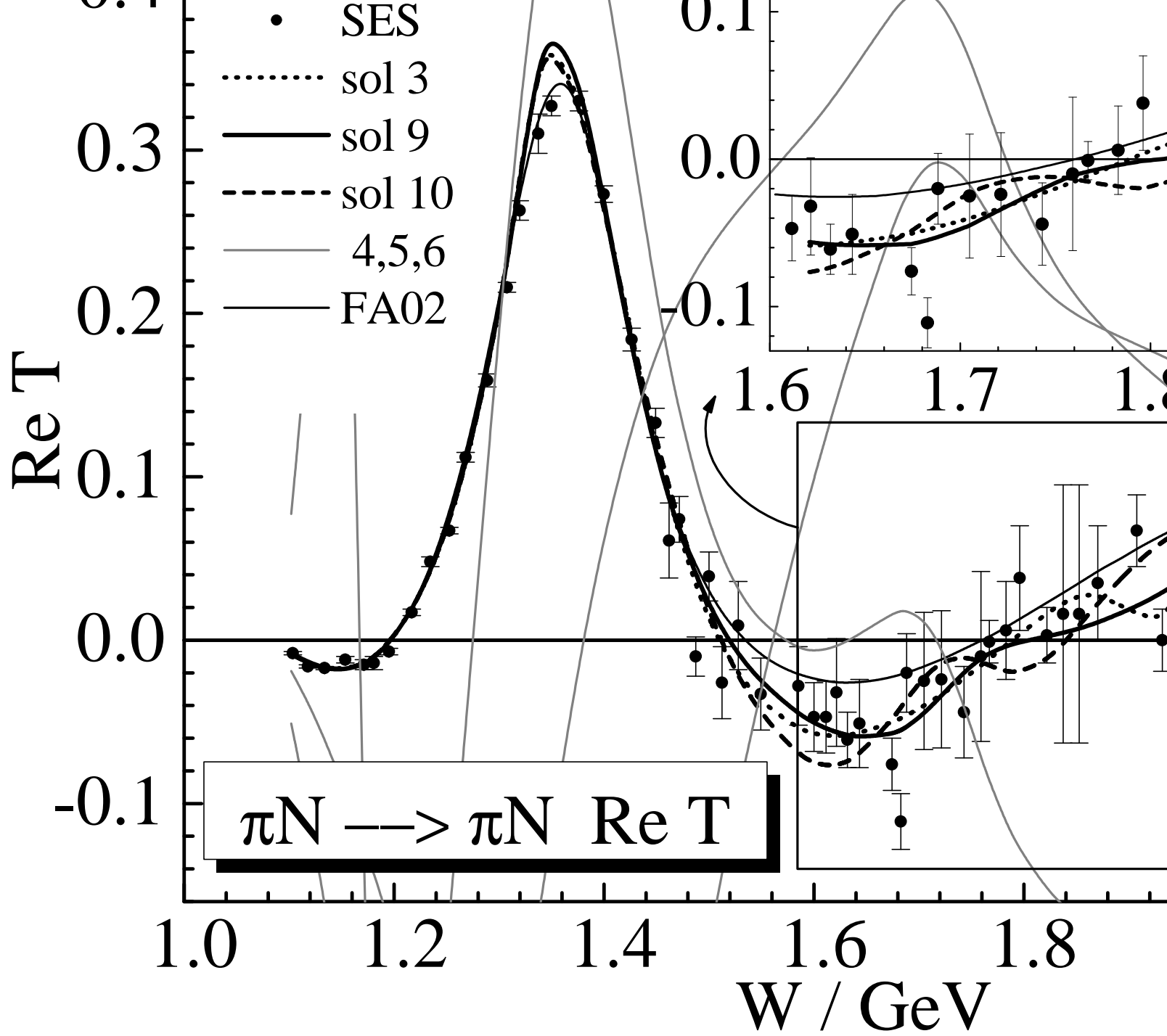
(b)

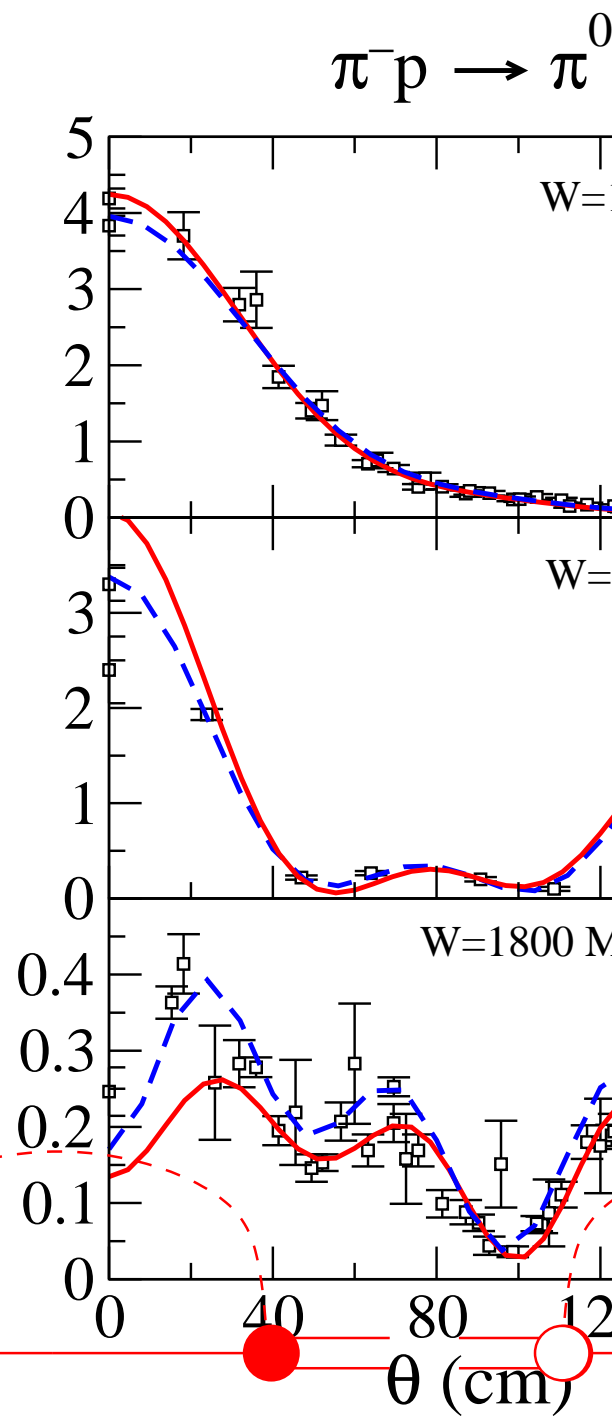
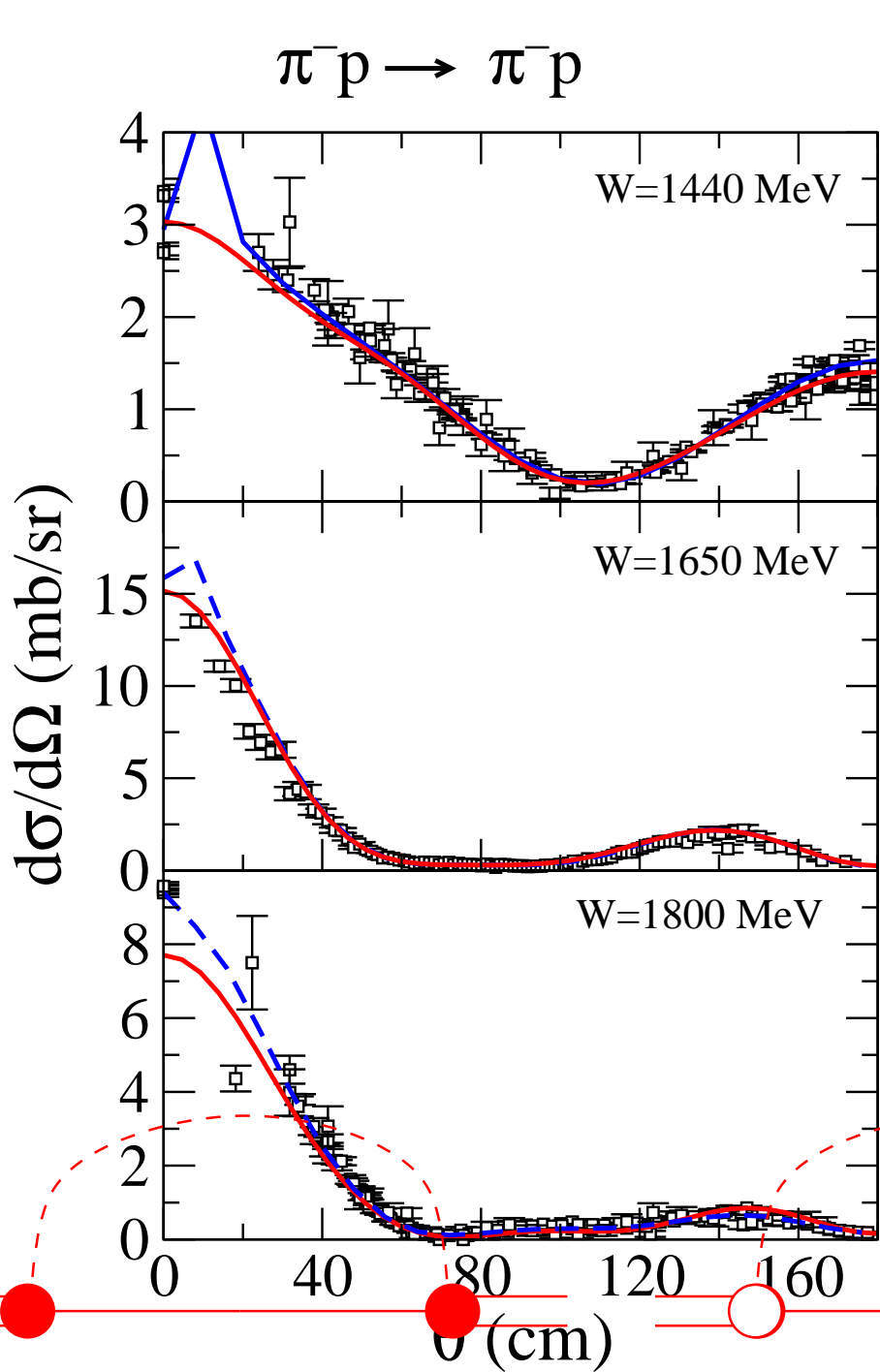


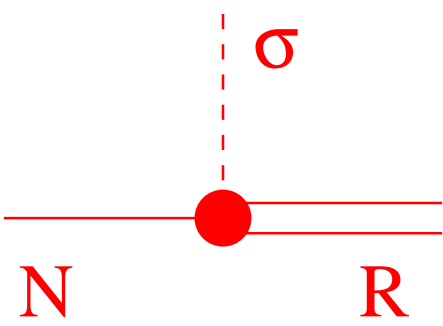
(c)



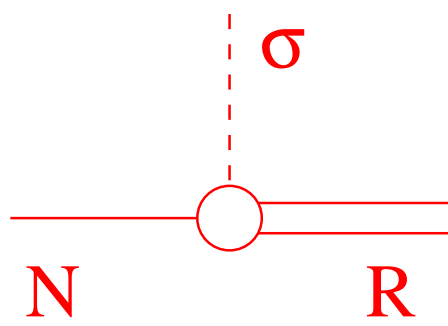
(d)



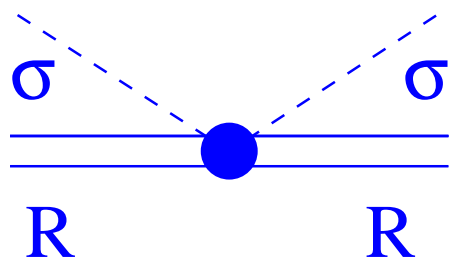




(a)



(b)



(c)